

# Nucleon Spin Structure Study at Jefferson Lab

Jian-ping Chen, Jefferson Lab, Newport News, VA 23606, USA

November 8, 2000

## Abstract

I will first review the latest development in the nucleon spin structure study with lepton-nucleon deep inelastic scattering (DIS) from high energy laboratories. I will then concentrate on the progress and plan of study of the nucleon spin structure in the low energy region. With the newly built high luminosity 6 GeV electron beam accelerator and the progress in the highly polarized electron source and highly polarized targets, new experiments are being carried out at Jefferson Lab (CEBAF) to study the nucleon spin structure in the resonance region at low  $Q^2$ , with focus on the generalized GDH sum rule. Some preliminary results are presented. A generalized GDH sum rule study could provide a first comparison of experimental data with calculations from a fundamental theory over the entire  $Q^2$  regime. Taking advantage of the high luminosity of Jefferson Lab, selected spin structure experiments in the DIS region are also planned, concentrating in the valence quark region and the study of the quark-gluon correlations through higher twist effects. The parton-hadron duality provides the link between the DIS and the resonance region. Experimental study of duality in spin structure is planned. Outlook of spin structure study with a future 12 GeV energy upgraded Jefferson Lab is discussed.

## 1 Introduction

In late 80s, the CERN European Muon Collaboration (EMC) spin structure experiment results [1], combined with earlier SLAC results [2], indicated that the quark spins contribute only a small amount to the nucleon spin. This puzzling situation is referred to as the “spin crisis”. Over the last decade,

both theoretical [3] and experimental physicists devoted substantial efforts to understand this problem. A new generation of experiments were carried out at SLAC (E142, E143, E154, E155 and E155x) [4], CERN (SMC) [5] and DESY (HERMES) [6]. These experiments concluded that the quark carries about 20 – 30% of the nucleon spin, and the Bjorken sum rule [7] is verified to about 7% level. The next section is an overview of the current status of the spin structure study.

At the  $Q^2 = 0$  end, there is another related sum rule for spin structure, the Gerasimov-Drell-Hearn (GDH) sum rule [8]. Large efforts have been put and are planned to test the GDH sum rule and to study the spin structure in the resonance region. In section 3, preliminary results from Mainz are presented as well as the future plans of Jefferson Lab and other laboratories.

To connect the GDH with the Bjorken sum rule, several attempts were made to extend the GDH sum rule. One of the generalized GDH sum rule derivation will be presented in Section 4. A large number of experimental efforts are underway at Jefferson Lab, which is a 100% duty factor 6 GeV electron accelerator with high luminosity. The recent progress in the polarized electron source and polarized proton, deuteron and  $^3\text{He}$  targets greatly extends the kinematic region for the study of the nucleon spin structure. First preliminary extended GDH experiment results with virtual photon are presented and discussed in Section 4.

Taking advantage of the high luminosity ( $10^{36}$  particles/sec for polarized beam-polarized target), experiments are planned at Jefferson Lab to study polarized valence quark structure with DIS in the high  $x$  region. As an example, one experiment, which will measure the neutron spin asymmetry ( $A_1^n$ ), is discussed in Section 6.

Experiments are also planned to study effects beyond the leading twist. The leading twist gives the quark distributions in the nucleon. The higher twists give access to the quark-gluon interactions. As an example, one experiment will measure the  $g_2$  spin structure function. The deviation of  $g_2$  from the leading twist part  $g_2^{ww}$ , which can be obtained from the measured  $g_1$  structure function, gives the twist 3 and higher twist contributions. Details are given in Section 7.

An energy upgrade to 12 GeV is planned for Jefferson Lab. Nucleon spin structure study with the upgraded Jefferson Lab is discussed in Section 8.

## 2 Overview of the nucleon spin structure study at high energy laboratories

### 2.1 Inclusive Polarized Lepton-Nucleon Scattering

High energy leptons provide a clean probe of the nucleon's substructure, since they only interact with quarks through the electroweak interaction (no strong interaction). Deep inelastic scattering of leptons with nucleons has provided us with the most extensive information on the parton substructure of the nucleon and helped to establish the current theory of the strong interaction, quantum chromodynamics (QCD), which is mostly responsible for the structure of the nucleon.

In the last 30 years, unpolarized lepton DIS has been successfully used to extract the parton distributions in the nucleon. The observation of the scaling violation over a wide kinematic range has confirmed QCD  $Q^2$  evolution. The polarized lepton DIS started in the 70s. A big surprise came in late 80s when EMC found that a quark-parton model (Ellis-Jaffe) sum rule[9] is violated and the quark spins do not account for the proton spin. This 'spin crisis' lead to great theoretical and experimental excitement. A number of new experiments at several high energy laboratories followed in the last decade. The new results from these experiments tested a rigorous QCD (Bjorken) sum rule, established the extent of the contribution of the quark spins to the nucleon spin and provided information on the polarized parton distribution, including a first glance at the gluon contribution to the nucleon spin.

For inclusive polarized lepton scattering off a polarized nucleon target, in the lowest order (first Born) approximation and neglecting the parity violating effect, the interaction is mediated by a virtual photon (with 4-momentum transfer  $Q^2$  and energy transfer  $\nu$ ). The cross section depends on four structure functions,  $F_1(Q^2, x)$ ,  $F_2(Q^2, x)$ ,  $g_1(Q^2, x)$  and  $g_2(Q^2, x)$ , where  $x = Q^2/2m\nu$  is the Bjorken scaling variable,  $F_1$  and  $F_2$  are the unpolarized structure functions and  $g_1$  and  $g_2$  are the polarized structure functions. In the Bjorken limit, when  $Q^2$  and  $\nu$  goes to  $\infty$  while the ratio  $x$  is kept constant, all structure functions become functions of  $x$  only, which is the Bjorken scaling behavior. In the naive quark-parton model,  $F_1$  and  $F_2$  give the quark momentum distribution and  $g_1$  gives the quark spin distribution:

$$g_1(x) = \frac{1}{2} \sum_i e_i^2 \Delta q_i(x) \tag{1}$$

where

$$\Delta q_i(x) = q_i^+(x) - q_i^-(x) + \bar{q}_i^+(x) - \bar{q}_i^-(x) \quad (2)$$

and  $q_i^+(x)(q_i^-(x))$  is the distribution of quark with flavor  $i$  and spin parallel (antiparallel) to the nucleon spin. The interpretation of  $g_2(x)$  in the QPM is less straight forward. It was shown that in QCD, it can be decomposed as

$$g_2(Q^2, x) = g_2^{WW}(Q^2, x) + \bar{g}_2(Q^2, x) \quad (3)$$

where  $g_2^{WW}$  is a leading twist contribution and is completely determined by  $g_1(Q^2, x)$ :

$$g_2^{WW}(Q^2, x) = -g_1(Q^2, x) + \int_x^1 g_1(Q^2, y) \frac{dy}{y}. \quad (4)$$

The term  $\bar{g}_2$  is a twist-3 contribution and is sensitive to the quark-gluon correlation in the nucleon.

The unpolarized cross sections are usually much larger than the polarized cross sections. Experimentally, it is usually easier to measure cross section asymmetries where the unpolarized part cancels. The experimentally measured asymmetries for a longitudinally polarized lepton beam on longitudinally and transversely polarized target are

$$A_{\parallel} = \frac{\sigma^{\uparrow\downarrow} - \sigma^{\uparrow\uparrow}}{\sigma^{\uparrow\downarrow} + \sigma^{\uparrow\uparrow}} \quad (5)$$

and

$$A_{\perp} = \frac{\sigma^{\downarrow\rightarrow} - \sigma^{\uparrow\rightarrow}}{\sigma^{\downarrow\rightarrow} + \sigma^{\uparrow\rightarrow}} \quad (6)$$

where the arrows in  $\sigma^{\uparrow\downarrow}$ ,  $\sigma^{\uparrow\uparrow}$ ,  $\sigma^{\downarrow\rightarrow}$ ,  $\sigma^{\uparrow\rightarrow}$  refer to the beam and target spin directions respectively. The physics asymmetries  $A_1$  and  $A_2$  are defined along and perpendicular to the virtual photon direction (the virtual photon-nucleon asymmetries).

$$A_{\parallel} = D(A_1 + \eta A_2) \quad (7)$$

and

$$A_{\perp} = d[A_2 - \gamma(1 - y/2)A_1] \quad (8)$$

where  $D$ , the depolarization factor of the virtual photon, depends on the kinematic variables and  $R$ , the ratio of unpolarized longitudinal cross section to the transverse cross section.  $\eta$  is a kinematic factor and  $d$  is proportional to  $D$ . For spin-1/2 targets (proton and neutron),

$$A_1 = \frac{\sigma_{1/2} - \sigma_{3/2}}{\sigma_{1/2} + \sigma_{3/2}} = \frac{2\sigma^{TT}}{\sigma_T} \quad (9)$$

and

$$A_2 = 2\sigma^{TL}/\sigma^T. \quad (10)$$

## 2.2 The Bjorken Sum Rule and Ellis-Jaffe Sum Rule

The sum rules of the spin structure functions relate the integral of the spin structure functions to some static properties of the nucleon. They provide powerful tools to experimentally test theoretical predictions. One fundamental sum rule is the Bjorken sum rule:

$$\int_0^1 g_1^p(x) dx - \int_0^1 g_1^n(x) dx = \frac{1}{6} \frac{g_A}{g_V} \quad (11)$$

where  $g_A$  and  $g_V$  are the axial and vector weak coupling constants measured from neutron beta decay. The sum rule was derived by Bjorken from light cone current algebra assuming isospin invariance. The modern day approach is using the QCD operator product expansion (OPE). The sum rule is valid at the  $Q^2 \rightarrow \infty$  limit. At finite  $Q^2$ , there are QCD radiative corrections:

$$\int_0^1 g_1^p(x) dx - \int_0^1 g_1^n(x) dx = \frac{1}{6} \frac{g_A}{g_V} \left[ 1 - \frac{\alpha_s(Q^2)}{\pi} - \dots \right] \quad (12)$$

where  $\alpha_s$  is the strong coupling constant.

Separate sum rules for the proton and the neutron were derived by Ellis and Jaffe within QPM, and assumed flavor-SU(3) symmetry and no strangeness contribution to the nucleon spin. Integration of eq. 1 gives

$$\Sigma^p = \frac{1}{2} \left( \frac{4}{9} \Delta u + \frac{1}{9} \Delta d + \frac{1}{9} \Delta s \right), \quad (13)$$

and, from isospin invariance,

$$\Sigma^n = \frac{1}{2} \left( \frac{1}{9} \Delta u + \frac{4}{9} \Delta d + \frac{1}{9} \Delta s \right), \quad (14)$$

where

$$\Delta q_i = \int_0^1 \Delta q_i(x) dx \quad (15)$$

are the moments of spin-dependent parton distributions in the proton. In the QPM, these moments are related to the weak axial-vector couplings  $a_0, a_3$  and  $a_8$ :

$$a_0 = \Delta u + \Delta d + \Delta s = \Delta \Sigma, \quad (16)$$

$$a_3 = \Delta u - \Delta d = \frac{g_A}{g_V}, \quad (17)$$

$$a_8 = \Delta u + \Delta d - 2\Delta s. \quad (18)$$

Assuming flavor-SU(3) symmetry,  $a_3$  and  $a_8$  are related to the symmetric and antisymmetric weak SU(3)<sub>f</sub> couplings F and D of the baryon octet,  $a_3 = g_A/g_V = F + D$  and  $a_8 = 3F - D$ . The measured F/D from the hyperon weak decay can be used to determine  $a_8$ . To determine  $a_0$ , Ellis and Jaffe assumed that the strange sea in the nucleon is unpolarized (i. e.  $\Delta s = 0$ ). therefore  $a_0 = a_8$ . The Ellis-Jaffe sum rule follows:

$$\Sigma^{p(n)} = \frac{1}{12}[+(-)a_3 + \frac{1}{3}a_8] + \frac{1}{9}a_0 = +(-)\frac{1}{12}(F + D) + \frac{5}{36}(3F - D). \quad (19)$$

The Ellis-Jaffe sum rule is valid in the  $Q^2 \rightarrow \infty$  limit. At finite  $Q^2$ , there are QCD radiative corrections, which are sizable in the  $Q^2$  range of the experiments.

Higher twist effects also contribute to the  $Q^2$  evolution of the  $g_1$  moments. It has been the subject of considerable theoretical effort. However, in the kinematics of most high energy spin structure experiments, these effects are believed not to be significant.

The  $Q^2$  evolution of the spin structure function  $g_1$  itself can be treated in perturbative QCD. The quark and the gluon distributions follow the Dokshitzer-Gribov-Lipatov-Altarelli-Parisi (DGLAP) equations[10]. Determination of the distribution functions depends on the renormalization and factorization scheme. The modified minimal subtraction ( $\overline{MS}$ ) scheme[11] and the Adler-Bardeen (AB) scheme[12] are commonly used in the analysis of the polarized parton distributions. In the  $\overline{MS}$  scheme, the gluon density  $\Delta G(Q^2, x)$  does not contribute to the first moment of  $g_1$ . In the AB scheme, the gluon density  $\Delta G(Q^2)$  contributes explicitly to  $\Sigma_1$  and the total quark contribution to the nucleon spin is  $Q^2$  independent.

### 2.3 Spin ‘Crisis’ and Recent Experimental Results

The EMC experiment result from CERN with polarized muon beam on polarized proton ( $\text{NH}_3$ ) target, when combined with the earlier results from SLAC E80 and E130, violates the Ellis Jaffe sum rule. The experimental result for  $\Sigma^p$  is  $0.126 \pm 0.010(\text{statistical}) \pm 0.015(\text{systematic})$ , while the Ellis-Jaffe sum rule prediction is  $0.189 \pm 0.005$ . The total quark contribution to the proton spin is only  $(12 \pm 9 \pm 14)\%$  and the strange sea quark contribution is  $-0.095 \pm 0.016 \pm 0.023$ . Such a small contribution of the quark spin to the proton spin came as a big surprise and was quoted as the ‘spin crisis’. It is clear now that it is only a ‘crisis’ of the quark model and the quark model still remains unjustified within QCD. However, the ‘spin crisis’ has generated much productive experimental and theoretical activity.

The 2nd generation of spin structure experiments were performed at SLAC (E142, E143, E154, E155 and E155x), CERN (SMC) and DESY (HERMES). The new generation experiments not only greatly improved the precision of the proton result, extended the kinematic coverage, but also measured on the deuteron and the neutron (with polarized  $^3\text{He}$ ). Some of the new generation of the experiments also measured both the longitudinal and the transverse asymmetries, which enabled the direct determination of  $g_1$  and  $g_2$ , instead of the early determination of  $g_1$  only from the longitudinal asymmetry with the assumption of  $g_2 = 0$ .

The latest results of  $g_1(x)$  for the proton, the deuteron and the neutron (from polarized  $^3\text{He}$ ) are summarized in figure 1[4]. Also for the first time, there are reasonable  $Q^2$  coverage that one can plot the  $Q^2$  evolution of the  $g_1^p(Q^2, x)$  structure function (see figure 2). Figure 3 shows the  $g_2(x)$  results for the proton and the deuteron.

With this reasonable amount of data, global QCD analyses have been carried out by several groups. Polarized parton distributions have been extracted from these analyses[13]. Precision data at very low  $x$  and high  $x$ , and wide  $Q^2$  range are needed to complete the picture and to have accurate determination of the complete parton distribution, especially the flavor and valence-sea separation and the polarized gluon distribution.

With all these results, the Bjorken sum rule is confirmed to about 7% and the Ellis-Jaffe sum rule is violated[14].

The determination of the total quark contribution to the proton spin is scheme dependent. Depending on which experimental data sets and which scheme ( $\overline{MS}$  and AB) are used, the results vary between 0.2 to 0.3 with

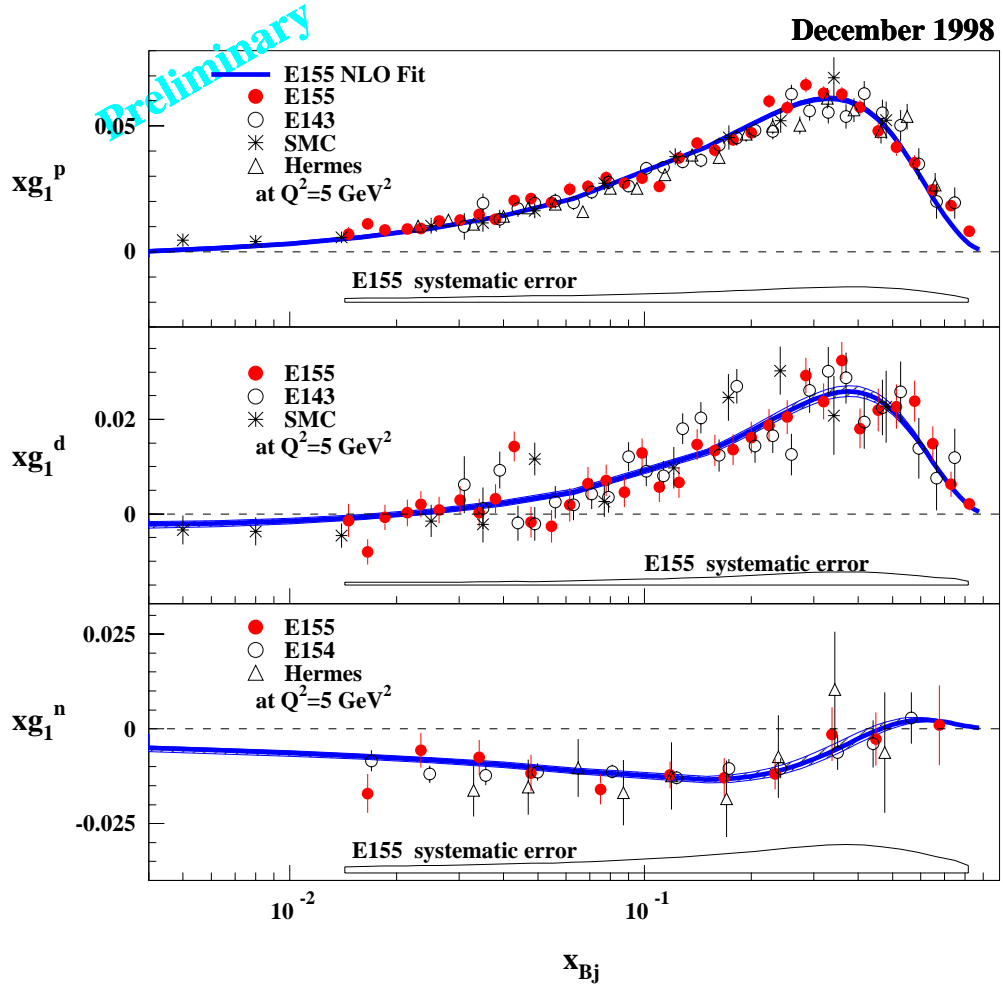


Figure 1: The preliminary result of  $g_1$  for proton, deuteron and neutron from SLAC experiment E155 and previous world data.

a typical uncertainty of 0.05. The remain contributions to the nucleon spin must come from the gluon contribution (including the gluon polarization and the gluon angular momentum) and the quark angular momentum. The same QCD analysis of the  $Q^2$  evolution gives an estimation of the polarized gluon distribution. SMC found the first moment of the polarized gluon distribution at  $Q^2 = 1\text{GeV}^2$  to be

$$\eta_g = \int_0^1 \Delta G(x) dx = 0.99_{-0.31}^{+1.17}(\text{stat.})_{-0.22}^{+0.42}(\text{syst.})_{-0.45}^{+1.43}(\text{theor.}). \quad (20)$$

The large uncertainties show that the indirect measurements have their lim-

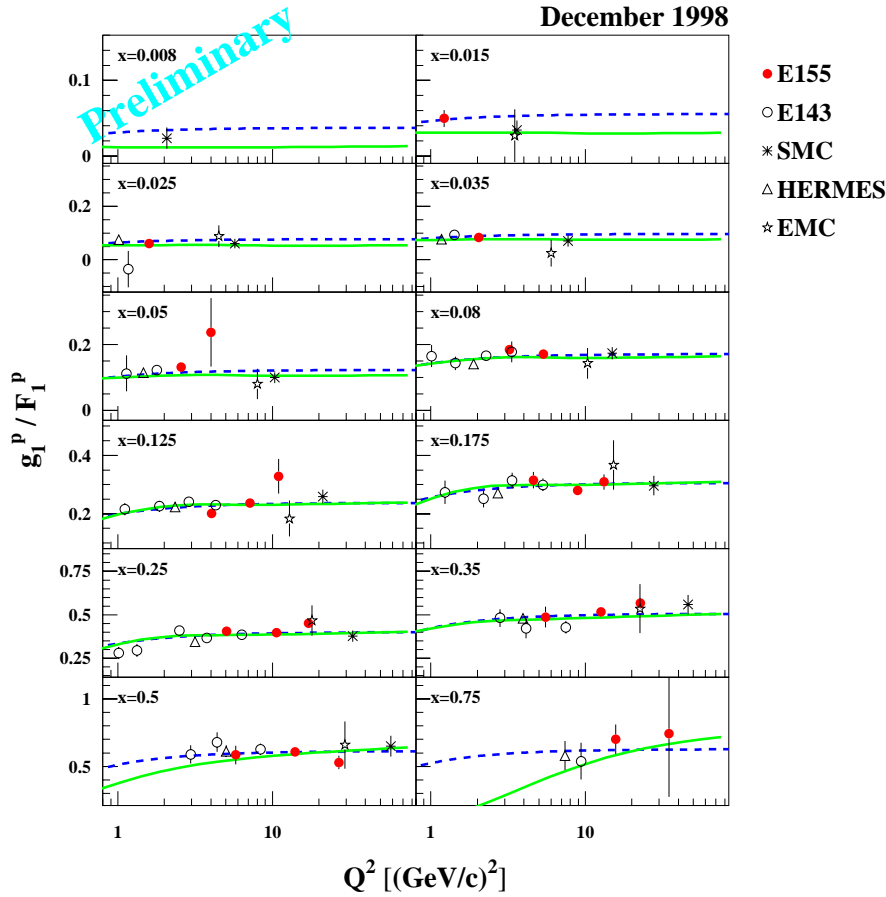


Figure 2: The preliminary result for the  $Q^2$  dependence of  $g_1^p$  from SLAC experiment E155 and previous world data.

itation and direct measurements are needed.

The gluon polarization has also been extracted from HERMES measurement of semi-inclusive asymmetry in the photoproduction of high  $p_T$  hadron pairs[15]. With a model-dependent analysis, HERMES determined that  $\Delta G/G = 0.41 \pm 0.18(stat.) \pm 0.03(syst.)$  at  $0.06 < x < 0.28$ .

Semi-inclusive experiments can provide the flavor decomposition. The first HERMES[16] and SMC[17] semi-inclusive results give the valence quark distributions and the sea quark distributions (assumed the flavor independence of the sea quark polarization). The first moments from HERMES data at  $Q^2 = 2.5 GeV^2$  are  $\Delta u + \Delta \bar{u} = 0.57 \pm 0.02 \pm 0.03$ ,  $\Delta d + \Delta \bar{d} = -0.25 \pm 0.06 \pm 0.05$  and  $\Delta s + \Delta \bar{s} = -0.01 \pm 0.03 \pm 0.04$ . With improved particle identification, HERMES will provide refined data for the flavor decomposition in near future.

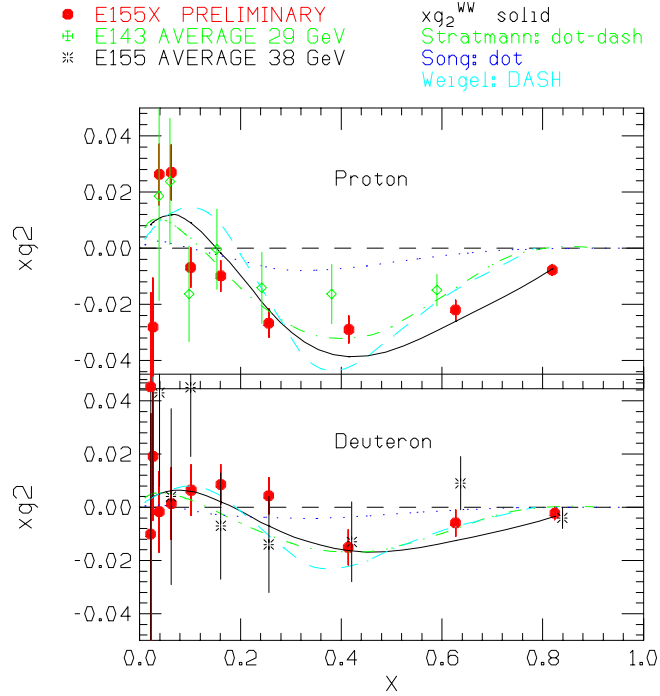


Figure 3: The preliminary result of  $g_2$  for proton and deuteron from SLAC experiment E155x and previous world data.

## 2.4 Future experiments

The large data sample provided by the high energy DIS experiments has allowed a reasonable determination of the polarized parton distributions. However, many questions remain to be answered.

One obvious piece in the proton spin puzzle is the polarized gluon contribution. Large experimental efforts are planned: RHIC-spin at Brookhaven, COMPASS at CERN, HERMES at DESY, and possibly others[18]. Results should be available in the next a few years.

Another piece in the proton spin puzzle is the quark angular momentum contribution. The theoretical study of this problem leads to a broad new framework which goes beyond the standard parton distribution functions: the generalized parton distributions (GPDs) (they are also called off-forward parton distributions or skewed parton distributions)[19]. The GPDs can be accessed with the deep virtual Compton scattering (DVCS) and the deep virtual meson productions. One of the GPD sum rules relates the quark angular momentum to the sum of one GPD[20]. Large efforts are planned at Jefferson Lab, HERMES, COMPASS to experimentally explore the GPDs. Several discussions are underway to build new facilities to study the GPDs. It is out of the scope of this paper to discuss these in great depth.

For inclusive lepton scattering measurements, the very low  $x$  region, the high  $x$  region and the  $Q^2$  dependence at all  $x$  regions are still to be explored. The high  $x$  region provides a clean region to study the valence quark structure. The  $Q^2$  dependence of the spin structure functions and the higher twist effects give access to the quark-gluon interactions. At low  $Q^2$  and  $Q^2 = 0$ , the focus has been on the study of the GDH sum rule, the generalized GDH sum rule and the resonance spin structure. Many experiments in a number of laboratories have been planned and some have been carried out. Efforts are also planned to study the connection between DIS and the resonance region (the parton-hadron duality).

New windows open up with the semi-inclusive reactions. The HERMES initial results are just the beginning of this new exploration. Further experiments in the semi-inclusive reactions will provide us with the complete spin-flavor decomposition of the spin structure. It can also access the transverse spin distribution[21], which is another important aspect of the nucleon spin structure.

### 3 Spin Structure with Real Photon: Gerasimov-Drell-Hearn Sum Rule

#### 3.1 The Gerasimov-Drell-Hearn Sum Rule

The Gerasimov-Drell-Hearn (GDH) sum rule[8] relates the total cross section of circularly polarized photons on longitudinally polarized nucleons to the anomalous magnetic moment of the nucleon:

$$\int_{thr}^{\infty} (\sigma_{1/2} - \sigma_{3/2}) \frac{d\nu}{\nu} = -2\pi^2 \alpha \frac{\kappa^2}{m^2} \quad (21)$$

where  $\sigma_{1/2}$  and  $\sigma_{3/2}$  are the total cross sections for hadron photoproduction on nucleons in the helicity 1/2 and 3/2 states,  $\nu$  is the laboratory photon energy,  $\kappa$  is the anomalous magnetic moment and  $m$  is the mass of the nucleon. The lower limit of the integration is the pion photoproduction threshold.

The GDH sum rule follows from the dispersion relation for forward Compton scattering along with the optical theorem and the low energy theorem. The forward Compton scattering amplitude may be written in terms of two scalar invariant functions of  $\nu$ :

$$f(\nu) = f_1(\nu) \vec{e}^{\prime*} \cdot \vec{e} + \nu f_2(\nu) i \vec{\sigma} \cdot \vec{e}^{\prime*} \times \vec{e} \quad (22)$$

where  $\vec{e}$  and  $\vec{e}'$  are the transverse polarization vectors of the incident and forward-scattered photon, respectively. Causality implies analyticity of  $f_2$  which allows us to write the dispersion relation for the forward amplitude without subtraction:

$$\text{Re} f_2(\nu) = \frac{2\nu}{\pi} \text{P} \int_0^{\infty} d\nu' \frac{\text{Im} f_2(\nu')}{\nu'^2 - \nu^2}. \quad (23)$$

Unitarity can be expressed in the optical theorem:

$$\text{Im} f_2(\nu) = \frac{\nu}{8\pi} (\sigma_{1/2} - \sigma_{3/2}) \quad (24)$$

The low energy theorem[22], which comes from gauge invariance and relativity, informs us that

$$f_2(0) = -\frac{\alpha \kappa^2}{2m^2}. \quad (25)$$

Combining the above equations, the GDH sum rule follows immediately. The no-subtraction assumption ( $\text{Re}(f_2(\infty)) = 0$ ) and that the cross section difference falls off with energy faster than  $1/\ln(\nu)$  could be open to ‘reasonable’ question. The GDH sum rule, especially the high energy behavior, can be used to study QCD and may have implications for physics beyond the Standard Model. The generality of the input assumption suggests very strongly that the sum rule should be verified, which has become possible now with the technical development in polarized beams, polarized targets and the new detection capabilities at Jefferson Lab, Mainz and other laboratories.

Because of the  $1/\nu$  weighting in the integrals, and that the resonances contribute most of the strength to the sum rule, single pion photoproduction is expected to have a sizeable contribution (dominant at low energy). Using the results of multipole analyses of the existing data, Karliner[23] and recently Workman and Arndt[24], Burkert and Li[25], Sandorfi, *et al.*[26], have computed the single pion contribution to the GDH sum rule for the proton and the neutron, with some estimates of the inelastic contribution included. These values are compared to the GDH prediction in table 1, along with the most recent calculation by Drechsel, Kamalov and Tiator[27] using an unitary isobar model (MAID), taking into account the single  $\pi$ ,  $\eta$  and double  $\pi$ ’s plus some estimation of the high energy contribution. Also listed are the values calculated based on an extended algebra model [28]. In the extended algebra calculation, the GDH sum rule is modified by extending the assumption of the ‘no-subtraction’ dispersion relation to have a  $J = 1$  pole contribution. However, recent analysis[29] suggests that the extra pole is not consistent with QCD analysis with existing data. Some of the analyses give reasonable agreement with the GDH sum rule for proton, but all missed the neutron GDH sum rule. It is of particular interest to notice that the proton-neutron sum rule (which is equivalent to isoscalar-isovector interference sum rule) is of different sign from the partial wave analysis results, and far from saturation by the existing calculation up to 2 GeV.

It is of great interest to experimentally test the GDH sum rule on both proton and neutron.

Recent theoretical efforts[29] provide extensive discussions on the subject of the GDH sum rule, including discussions of the validity of the no-subtraction hypothesis, the consequences of the GDH sum rule for our understanding of the nucleon structure, the strong interaction (QCD) and possible new physics beyond the Standard Model, and the estimation of the high energy ( $\mu > 2$  GeV) contribution.

Table 1. Various Predictions for GDH sum

-	GDH(p)	GDH(n)	GDH(p-n)
GDH sum rule	-204.5 $\mu\text{b}$	-232.8 $\mu\text{b}$	28.3 $\mu\text{b}$
Extended Current Algebra	-294 $\mu\text{b}$	-185 $\mu\text{b}$	-109 $\mu\text{b}$
Analysis by Karliner	-261 $\mu\text{b}$	-183 $\mu\text{b}$	-78 $\mu\text{b}$
Analysis by Workman and Arndt	-257 $\mu\text{b}$	-189 $\mu\text{b}$	-68 $\mu\text{b}$
Analysis by Burkert and Li	-203 $\mu\text{b}$	-125 $\mu\text{b}$	-78 $\mu\text{b}$

### 3.2 First Measurement of GDH integral on Proton: Preliminary Result from Mainz

The first GDH experiment was carried out at the Glasgow-Mainz tagged photon facility of the MAMI accelerator in Mainz, Germany[32]. Circularly polarized photons are produced by bremsstrahlung of longitudinally polarized electrons with energy up to 800 MeV. A strained GaAs photocathode routinely delivered electrons with polarization of about 75%. The electron polarization was monitored with a Møller polarimeter to a precision of 3%. The photon polarization was evaluated according to Ref [33]. The photon energy was determined by a tagging spectrometer which analyzes the momenta of the electrons which have radiated bremsstrahlung photons.

A frozen spin butanol ( $\text{C}_4\text{H}_9\text{OH}$ ) target provided the polarized protons. The system consisted of a horizontal dilution refrigerator and a 2.5 Teslas superconducting magnet, used in the polarization phase, together with a microwave system for dynamical nuclear polarization. During the measurement the polarization was maintained in the frozen-spin mode at a temperature of about 50 mK and a magnetic field of 0.4 Tesla. A maximum polarization close to 90% and a relaxation time in the frozen-spin mode of about 200 hours have been regularly achieved. The target length of 2 cm gave a total thickness of  $9 \times 10^{22}$  protons/cm<sup>-2</sup>. The target polarization was measured with NMR techniques to a precision of 1.6%.

A large angular acceptance ( $21^\circ < \theta < 159^\circ$ ; full azimuthal angle coverage) detector DAPHNE, complemented by additional detectors covering the forward angular region down to  $2^\circ$ , were used to detect the photoemitted hadrons. Preliminary data discussed below are data recorded only by the DAPHNE detector. The forward angle data are still under analysis.

The experiment measured inclusive hadron production (count of hadron events without partial channel separation) and the exclusive channels (single

pion production and double pion production) for photon energies from 200 MeV to 800 MeV. Preliminary results of the inclusive cross section difference and the GDH integral have already been shown at conferences[32]. The experimental systematic uncertainty is about 6%. The uncertainty due to the angular extrapolation is not significant and will be checked once the forward angle data analysis is complete. The total measured sum in the range of 200-800 MeV is  $I_{GDH}^p = 216 \pm 6(stat.) \pm 13(syst.)(\mu b)$ . The region below 200 MeV and above 800 MeV will be measured in other laboratories and the contributions have been estimated with models. It is worth mention that the contribution from the pion threshold to 200 MeV is important and with opposite sign (from the resonance contribution).

The double polarization data can be also used to extract the spin polarizability  $\gamma_0$ , which is defined to be

$$\gamma_0 = -\frac{1}{4\pi} \int_{m_\pi}^{\infty} \frac{(\sigma_{3/2} - \sigma_{1/2})}{\nu^3} d\nu. \quad (26)$$

The measured integral in the region of 200-800 MeV is  $I_{\gamma_0} = 170 \pm 9 \pm 10(10^{-6} fm^4)$ . The contribution from the unmeasured region can be estimated with models[34] Adding the estimation to the measured contribution, one gets the spin polarizability  $\gamma_0 = -83 \pm 9 \pm 15(10^{-6} fm^4)$ , which is to be compared with Chiral perturbation calculations[35]. The latest Chiral perturbation calculation to order of  $p^4$  by Gellas-Hemmert-Meissner gives a result of  $\gamma_0 = -110(10^{-6} fm^4)$ .

### 3.3 Planned Experiments on Real Photon GDH

The first measurement at Mainz is part of the joint program to experimentally test the GDH sum rule on the nucleon at MAMI and ELSA (Bonn)[36]. The photon energy range covered at ELSA is from 600 MeV to 3 GeV. The same polarized butanol target will be used for the proton measurement, which is scheduled to start data taking this year. The ELSA experiment will be only an inclusive measurement. Extension of the measurements to the neutron using both polarized deuteron and polarized  $^3\text{He}$  targets is approved for MAMI[37] and is under discussion for ELSA.

There are two planned Jefferson Lab experiments (E91-015[38] and E94-117[39]) will use polarized real photon on a polarized ice HD target and CLAS (CEBAF large acceptance spectrometer) to study the proton and the neutron (with deuteron) GDH sum rule and also all the exclusive channel

contributions for photon energies from 300 MeV to 2.2 GeV and can be extended to 6 GeV. The polarized ice HD target is a novel new target which provides a relatively ‘clean’ Hydrogen and Deuterium target. The target is being built at Brookhaven first for the LEGS-Spin program. It will later be used for the Jefferson Lab GDH program.

Similar studies at different photon energies are also planned at LEGS[40], Grenoble[41], Spring8[42] and TUNL[43].

## 4 Spin Structure with Virtual Photons: Generalized GDH Sum Rule

The nucleon spin structure has been explored for more than two decades at high energies. However, the exploration with real photons has just started and the transition from the deep inelastic regime to the confinement regime has not been explored at all. The connection between the GDH and the Bjorken sum rules may provide insight into how this transition takes place.

Trying to better understand the “spin crisis” and to learn about the possible higher twist effects from the  $Q^2$  dependence of the spin structure functions, phenomenological models have been proposed to extend the GDH sum rule for the nucleon to finite  $Q^2$  and connect it to the Bjorken sum rule in deep inelastic regime [44, 45, 46]. A natural extension will be

$$I(Q^2) = \int_{threshold}^{\infty} \frac{\sigma^{1/2}(\nu, Q^2) - \sigma^{3/2}(\nu, Q^2)}{\nu} d\nu. \quad (27)$$

However, what does this integral equal to is not defined. Therefore it is only an extended GDH integral, not a sum rule. Recently Ji and Osborne[48] has made a rigorous extension of the GDH sum rule to the entire region of  $Q^2$ . With the same assumptions as the GDH sum rule, Ji and Osborne derived the generalized GDH sum rule:

$$4 \int_{el}^{\infty} \frac{G_1(\nu, Q^2)}{\nu} d\nu = S_1(Q^2) \quad (28)$$

where  $S_1(Q^2)$  is the forward virtual Compton Scattering amplitude. Similar sum rule also holds for  $G_2$  and  $S_2$ . The GDH sum rule and Bjorken sum rule are the two limiting cases ( $Q^2 = 0$  and  $Q^2 = \infty$ ) of the generalized GDH sum rule. Other than the two limiting cases,  $S_1(Q^2)$  can also

be calculated at small  $Q^2$ , where hadrons are the relevant degree of freedom, with Chiral Perturbation Theory and at large  $Q^2$ , where quarks and gluons(partons) are the relevant degree of freedom, with higher order QCD expansion (twist expansion). At small  $Q^2$ , it was first calculated to the leading order[47][48] using the Chiral Perturbation theory with the Heavy Baryon approximation. However, the calculated slope has an opposite sign from the constituent quark model calculations. Recently the calculation was extended to next to leading order (order  $P^4$ )[49]. The slope now has the same sign as the constituent quark model calculations. A new improved calculation without Heavy Baryon approximation is under way [50]. At large  $Q^2$ , twist-2 and twist-4 terms have been calculated[51]. A crucial question in this connection is how low in  $Q^2$  the Bjorken sum rule can be evolved using the high twist expansion? Recent estimates [51] suggest as low as  $Q^2 = 0.5 \text{ GeV}^2$ , since the expansion scale is the quark transverse momentum ( $p_T \approx 0.3 \text{ GeV}$ ). Also at the other end, chiral perturbation theory may allow evolution of the GDH sum rule to  $Q^2 = 0.2 \text{ GeV}^2$  or higher. Theoretical efforts (such as lattice calculations) are needed to bridge the remaining gap.

*The importance of such efforts cannot be overemphasized as it would mark the first time that hadronic structure is described by a fundamental theory in the entire kinematics regime, from short to large distances.*

Experiments have been carried out at JLAB on polarized  $NH_3$ [52],  $ND_3$ [53], and  $^3He$ [54] targets to extract the  $Q^2$  evolution of the GDH integral for protons and neutrons in a range of  $Q^2 = 0.1 - 2.0 \text{ GeV}^2$  and from the elastic to the deep inelastic regime. Results on the Sum Rule are expected shortly. Figure 4 shows some preliminary asymmetry results from the experiment on polarized  $^3He$ . Both parallel (target polarized along beam direction) and perpendicular (target polarized perpendicular to the beam direction) asymmetries are measured. The virtual photon asymmetries  $A_1$  and  $A_2$  were extracted and are shown in figure 4. The  $A_1$  asymmetries are positive in the quasielastic peak, negative in the  $\Delta$  region, and become small in the higher mass resonances. Contrast to high energy case, the  $A_2$  asymmetries are not negligible at low energies. Combining these asymmetries with cross sections, one can extract the spin structure functions  $g_1$ ,  $g_2$  and the generalized GDH sum integrals.

A new experiment[55] will extend the range down to very low  $Q^2$  (below  $0.02 \text{ GeV}^2$ ) and to higher virtual photon energies in order to extrapolate to the real GDH sum rule (see figure 5).

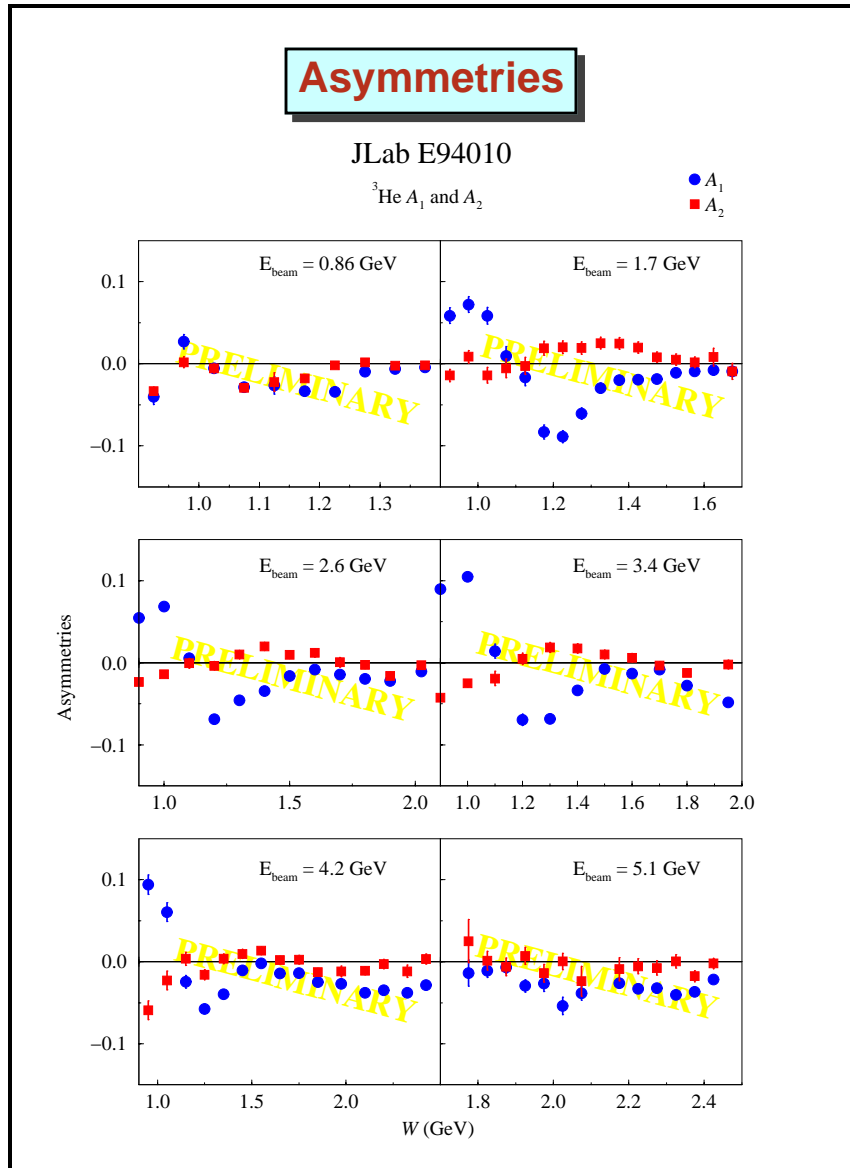


Figure 4: Preliminary results of spin asymmetries from JLab E94-010

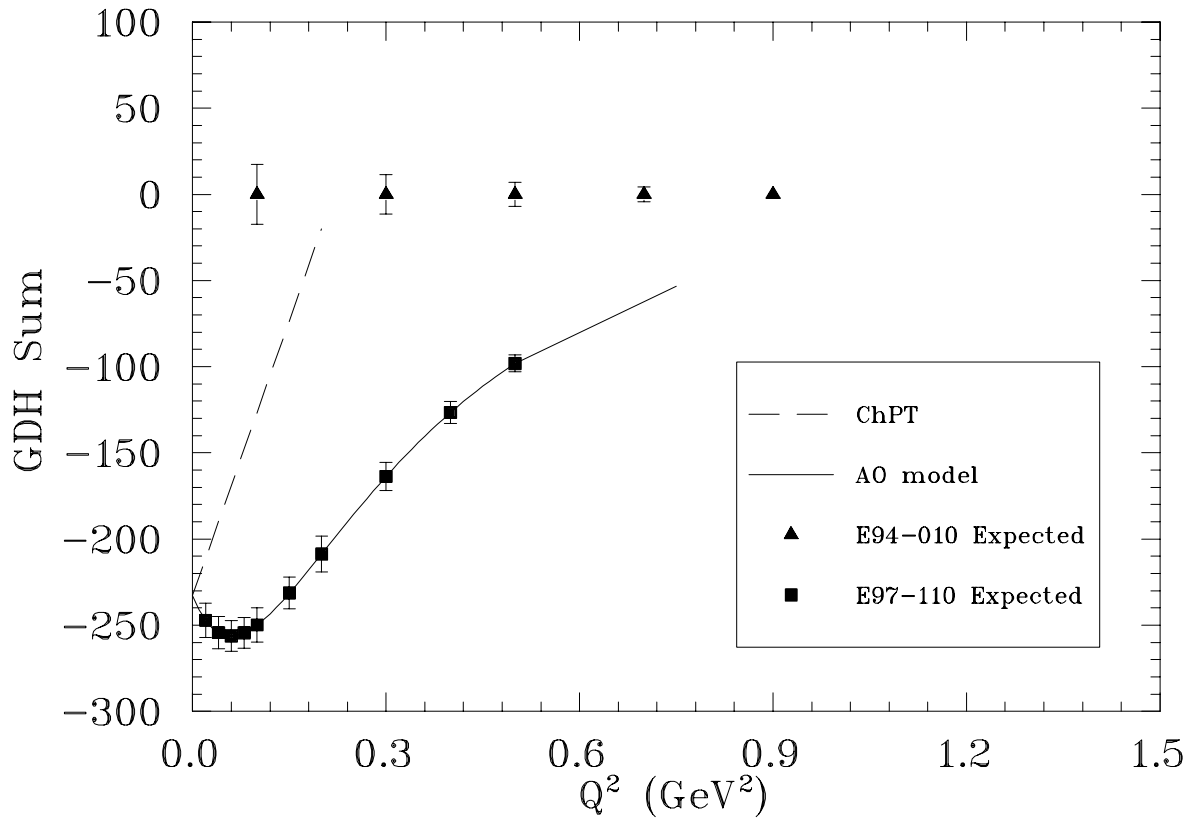


Figure 5: JLab E97-110 and E94-010 expected extended GDH sum results

The GDH sum rule and its  $Q^2$  dependence for  $^3\text{He}$  itself is of great interest. However, at the same time we can extract information on the neutron. To extract the sum rule for the neutron from the measured data for the  $^3\text{He}$ , we need to take into account the fact that the polarized  $^3\text{He}$  is only approximately a polarized neutron target[56]. We need to subtract the contribution from the small proton polarization and take into account that the neutron is not polarized to the same level as the  $^3\text{He}$  itself.

The first order correction can be made by using the calculation of Friar *et al.*[56] that the proton is about 3% polarized in the opposite direction from the  $^3\text{He}$  polarization, while the neutron is about 87% polarized along the  $^3\text{He}$  polarization direction.

Recently degli Atti and Scopetta[57] suggested to use the following equation to extract neutron sum rules:

$$\tilde{I}^n(Q^2) = \frac{1}{p_n} [I^{^3\text{He}}(Q^2) - 2p_p I^p(Q^2)] \quad (29)$$

where  $p_{n(p)}$  is the effective nucleon polarization, produced by the  $S'$  and  $D$  waves in the ground state of  $^3\text{He}$ . It was shown that, even though the quantity  $\tilde{g}_1^n(x, Q^2)$  differs significantly from  $g_1^n(x, Q^2)$  at the resonance region at low  $Q^2$ , the difference for the integrated quantity  $\tilde{I}^n(Q^2)$  does not differ much from the free neutron sum rule  $I^n(Q^2)$  (at most 10%).

More realistic  $^3\text{He}$  models can be used to further study the  $^3\text{He}$  GDH sum rule and the extraction of the neutron sum rule. Several theorists are investigating this problem[58].

## 5 Spin Structure in the High $x$ Region

Deep Inelastic Scattering (DIS) has been one of the most successful probes of nucleon structure. Since the late 1960s, unpolarized DIS has established the quark-parton picture of the nucleon structure. The parton (valence quarks, sea quarks and gluon) distribution functions have been extracted with global QCD analysis[59]. Extensive data of  $F_2(x, Q^2)$ , measured over several orders of magnitude in  $Q^2$  and  $x$  ranges, are in excellent agreement with the QCD evolution, providing one of the most convincing evidence in support of QCD. As reviewed in section 1, after the ‘spin crisis’, substantial effort has been devoted over the last decade on polarized DIS experiments and has provided us with rich information on the nucleon spin structure. Extraction of the

polarized parton distribution functions have been attempted. The uncertainties are much larger compared with the unpolarized parton distribution functions due to the fact that the polarized data coverage is not as extensive as the unpolarized data. Most of the polarized DIS experiments were focussed on measurements of the first moment of the spin structure function and on testing spin sum rules, which require an accurate determination of the distributions at small values of  $x$ ,  $x < 0.2$ , where sea quarks and antiquarks are dominant. On the other hand, we do not yet have a good determination of the spin-dependent valence quark distributions in the region where a quark carries a large fraction of the nucleon's momentum (high  $x$ ). Unlike sea quarks, which are largely generated in perturbative QCD through gluon bremsstrahlung and subsequent splitting into quark-antiquark pairs, valence quarks are entirely non-perturbative, and therefore more directly reflect the structure of the QCD ground state [60].

The lack of data in the valence region is particularly glaring in the case of the neutron, where there is no information at all on the spin structure function beyond  $x \sim 0.5$  (see figure 6). Knowledge of the neutron structure function is essential for understanding how the various quark flavors are polarized. The proton structure function at large  $x$  provides one particular linear combination of the valence  $\Delta u$  and  $\Delta d$  distributions, however, to solve for  $\Delta u$  and  $\Delta d$  separately requires a second independent combination, such as that afforded by the neutron.

## 5.1 Physics in the high $x$ region

To first approximation, the constituent quarks in the nucleon are described by the SU(6) wavefunctions. Isospin and SU(6) symmetries lead to the three predictions:

$$R^{np} = \frac{F_2^n}{F_2^p} = \frac{2}{3}; \quad A_1^p = 5/9; \quad \text{and} \quad A_1^n = 0. \quad (30)$$

Data for  $A_1^p$  and  $A_1^n$  are shown in figure 6. A qualitative success of SU(6) is displayed in the region  $x > 0.4$ , for  $A_1^p(x)$ , where the data is consistent with  $5/9$ . Also  $A_1^n(x)$  is consistent with being small (but negative) everywhere. On the other hand, data for  $R^{np}$  shown in figure 7 agree poorly with the SU(6) prediction.  $R^{np}(x)$  is a straight line but with a big slope starting with  $R^{np}(0) = 1$  but dropping to approximately  $R^{np}(1) = 1/4$ . The behavior of

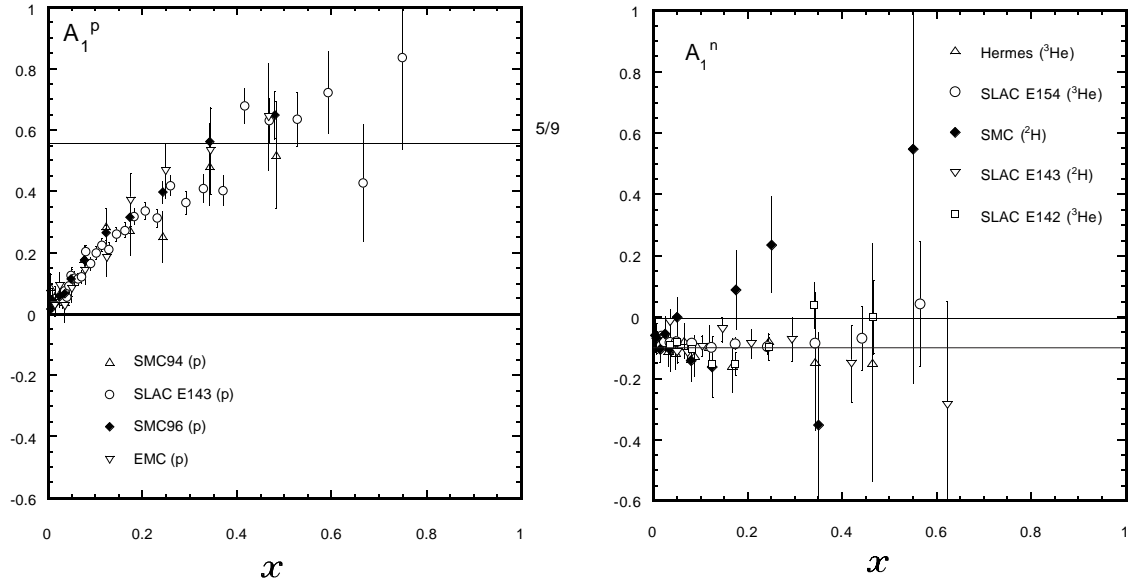


Figure 6: Left: World proton data  $A_1^p$  versus  $x$ . Right: World neutron data  $A_1^n$  versus  $x$ .

$R^{np} \sim 1$  and  $A_1^p \sim 0$  at small values of  $x$  may be explained by the presence of sea quarks, which are not expected to have SU(6) symmetry. At high  $x$ , where the sea quark contributions are small, the behavior of  $R^{np}$  is a clear sign of SU(6) symmetry broken for valence quarks.

A natural explanation based on phenomenological arguments [61, 62] is an SU(6)-breaking suppression of the “diquark” configurations  $S = 1$  relative to the  $S = 0$  configuration. The dynamical origin of the SU(6) breaking could come from a large hyperfine interaction among the quarks:

$$\vec{S}_i \cdot \vec{S}_j \delta^3(\vec{r}_{ij}). \quad (31)$$

It is this interaction that explains, for example, the  $N - \Delta$  splitting. The effect of the perturbation on the wavefunction is to have the  $S = 0$  “diquarks” term to dominate at high  $x$ . The dominance of this term as  $x \rightarrow 1$  implies:

$$R^{np} \rightarrow \frac{1}{4}; \quad A_1^p \rightarrow 1; \quad \text{and} \quad A_1^n \rightarrow 1. \quad (32)$$

If indeed this specific SU(6) symmetry breaking is the explanation for the behavior of  $R^{np}(x)$ , then there are also predictions for  $A_1^p(x)$  and  $A_1^n(x)$

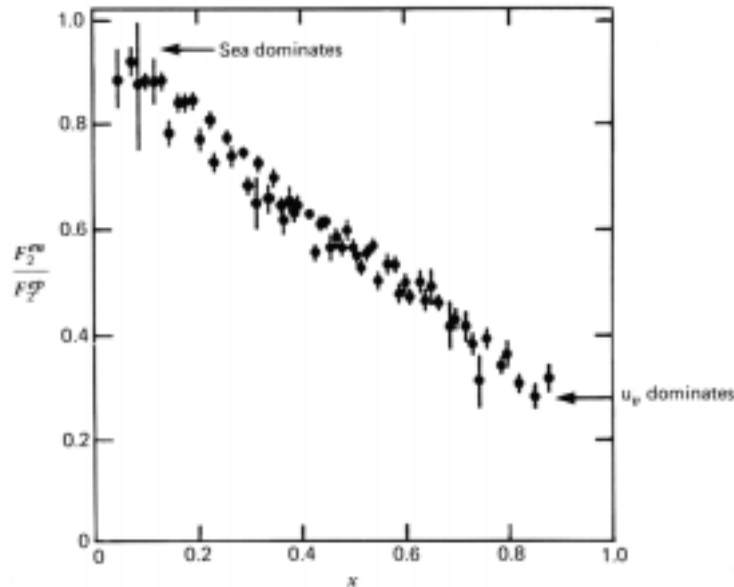


Figure 7:  $F_2^n/F_2^p$  as a function of  $x$  ratio extracted from the SLAC measurements of proton and deuteron in unpolarized deep inelastic scattering.

as shown in figure 8. As recently pointed out by Isgur [63], there is little freedom in the predictions if quarks with broken SU(6) symmetry are a useful description of the nucleon. Unfortunately, the data on  $A_1^{n,p}$  at high  $x$  lacks the precision even to distinguish this prediction from the simple SU(6) prediction.

Another approach focuses directly on relativistic quarks instead of the nonrelativistic quarks of the above discussion. Farrar and Jackson[64] in the early 70's, as one of the first applications of pQCD, noted that at  $x \rightarrow 1$ , the scattering is from a high energy quark, and the process can be treated perturbatively. Farrar and Jackson proceeded to show that a quark carrying nearly all the momentum of the nucleon (i.e.  $x \rightarrow 1$ ) must have the same helicity as the nucleon and that quark-gluon interactions cause only the  $S = 1$ ,  $S_z = 1$  diquark spin projection component, rather than the full  $S = 1$  diquark system to be suppressed as  $x \rightarrow 1$ . While starting with an SU(6) wave function they break the SU(6) symmetry in the dynamics describing the transfer sharing through gluon exchange in the diquark system. The authors found similar limiting values when  $x$  approaches unity as previously for both the proton and the neutron, namely  $A_1^{n,p} \rightarrow 1$  for  $x \rightarrow 1$ . Note that in this theory  $R^{np} \rightarrow 3/7$  versus  $1/4$  for the constituent quarks. A similar

result is obtained in the treatment of Brodsky and collaborators [65] based on quark-counting-rules. This is one of few places where QCD can provide for an absolute prediction about structure functions (here a ratio of structure functions). How low in  $x$  this picture works is uncertain.

Recently, Boglione and Leader [66] used fits to the world unpolarized and polarized data with two constraints one being the Soffer bound and the other the pQCD results when  $x$  approach unity to make specific predictions for the behavior of  $A_1^n$  and  $A_1^p$  over the full range of  $x$ . Depending on the polarized distribution they use, the result is dramatically different in the large  $x$  region for the neutron.

Finally, we note also that Kochelev [67] has proposed an approach to interpreting the nucleon within QCD that includes instantons as an important degree of freedom. With this radically different picture, the prediction is that  $A_1^n(x)$  remains close to zero.

## 5.2 Planned measurement of $A_1^n$ at high $x$

An experiment JLab E99-117[68] is planned at JLab for next year to measure  $A_1^n$  in the  $x$  region from 0.33 to 0.63 with high precision. The experiment will use a highly polarized (80%) 6 GeV electron beam on a high pressure ( $> 10$  atm.) highly polarized (40%)  $^3\text{He}$  target. Scattered electrons will be detected with two high precision spectrometers with their associated detectors.  $A_1^{^3\text{He}}$  will be measured with high precision. The extraction of the neutron information from the measurement with a polarized  $^3\text{He}$  target has been studied by several groups[69]. The effect is negligible in the region of  $x$  less than 0.8. Figure 8 shows the projected results for  $A_1^n$  measurements with 11 GeV beam. The first experiment with 6 GeV beam will cover the part below  $x = 0.63$ . These results will determine if  $A_1^n$  will cross zero to become positive or not, therefore will determine if the predictions by the constituent quark models and pQCD are valid.

A new proposal[70] will extend the measurements into resonance region to test if the quark-hadron duality works for the spin structure functions ( $g_1$  and  $A_1$ ). The duality has been established for the spin independent structure functions ( $F_1$  and  $F_2$ ). But has never been tested for the spin structure functions. If it does work for the spin structure functions, it can be used to greatly extend our  $x$  region to very high  $x$  to help study the physics at  $x \rightarrow 1$  limit.

To further understand strong interaction and the quark-gluon structure

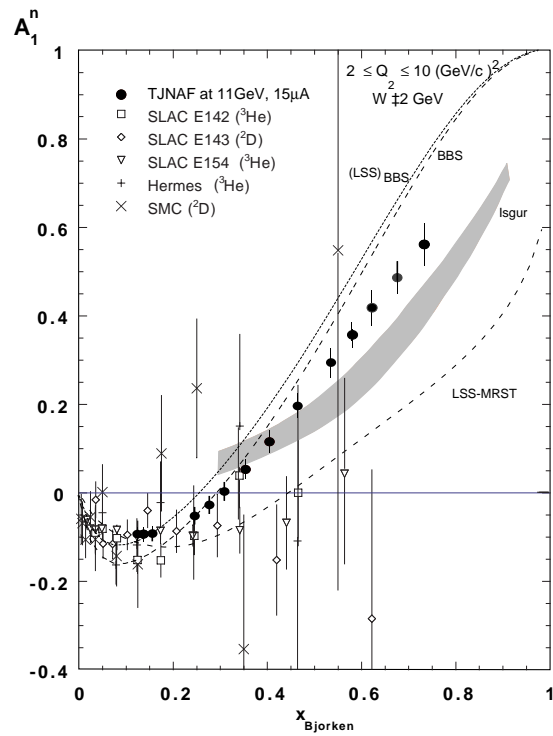


Figure 8: The World data of  $A_1^n$  neutron versus  $x$  and the projected data for JLab 11 GeV.

of the baryon and meson, an energy upgrade to 11-12 GeV has been proposed for the CEBAF machine at JLab. With high luminosity 11 GeV, JLab will be the best place to study physics in the high  $x$  region. The figure of merit will be at least two orders of magnitude better than other existing high energy laboratories. A proposal [71] to perform high precision measurement of  $A_1^n$  at large  $x$  region is one of the ‘key’ experiments for the JLab upgrade. Figure 8 shows the projected results along with the world data and theoretical predictions. This experiment will undoubtedly give us insight into the dynamics of partons in the nucleon.

## 6 Higher twist effects: $g_2$ structure function

The spin structure function  $g_1$  has a simple interpretation in the quark-parton model and provides direct information about the spin distribution in terms of its constituent quarks. On the other hand,  $g_2$  does not have a simple interpretation in the quark-parton model due to its unique sensitivity to the so called “higher twist effects”. These higher twist effects describe physics beyond the simple parton distributions, such as quark-gluon correlations, which are not present in the naive quark-parton model descriptions of the nucleon structure.

### 6.1 Introduction to high twist effects

Most of the known higher-energy processes can be understood in terms of the quark-parton model which describes the scattering in terms of *incoherent* parton scattering. On the other hand, the higher-twist processes cannot be understood in terms of the simple parton model. Rather, one has to consider parton correlations initially present in the participating hadrons, which means that the associated process is *coherent* in the sense that more than one parton from a particular hadron takes part in scattering. As such, higher-twist observables are exceedingly interesting because they provide the unique opportunity to study the quark and gluon correlations in the nucleon which cannot otherwise be accessed.

In general, however, higher-twist processes cannot be cleanly separated from the leading twist because of the so-called infrared renormalon problem. However, the  $g_2$  structure function is an exception because it contributes at the leading order to the twist-3 effect after subtracting a piece from  $g_1$

contribution. Therefore,  $g_2$  is among the *cleanest* higher-twist observables.

## 6.2 Operator Product Expansion and Moments of $g_2$

The concept of twist comes from using the Operator Product Expansion (OPE) to describe the matrix element for the virtual Compton scattering process [72],

$$\langle PS | [J(\xi)J(0)] | PS \rangle,$$

where  $P$  and  $S$  are the hadron four-momentum and spin, and  $J(\xi)J(0)$  is a product of the unknown hadron currents. This product of currents is expanded in a Taylor's series of operators and unknown coefficients that describe the various quark and gluon interactions within the nucleon, and the relative strength of these interactions respectively. In this expansion, terms are grouped together according to their degree of singularity in the scaling limit, which corresponds to physics at the light-cone ( $\xi^2 \rightarrow 0$ ). The degree of singularity of a given term is labelled by a quantity known as the *twist*  $\tau$ , with the most singular (and therefore most dominant) contributions having twist  $\tau = 2$ . Higher-twist terms, which contain information about quark-gluon correlations, are suppressed by additional factors of  $1/Q$  relative to the leading twist contribution. If we assume that terms with  $\tau \geq 4$  can be neglected for reasonably large values of  $Q^2$ , the OPE allows one to relate the moments of the spin structure functions  $g_1(x, Q^2)$  and  $g_2(x, Q^2)$  to the matrix elements of the  $\tau = 2$  and  $\tau = 3$  operators,

$$\int_0^1 x^j g_1(x, Q^2) dx = \frac{a_j(Q^2)}{2}, \quad j = 0, 2, 4, \dots$$

$$\int_0^1 x^j g_2(x, Q^2) dx = \frac{1}{2} \frac{j}{j+1} [d_j(Q^2) - a_j(Q^2)], \quad j = 2, 4, \dots$$

where the  $a_j(Q^2)$  are twist-2 matrix elements, and the  $d_j(Q^2)$  are twist-3 matrix elements. Combining the above expressions, one can write the following expression for  $d_j$

$$d_j(Q^2) = 2 \int_0^1 x^j \left[ g_1(x, Q^2) + \frac{j+1}{j} g_2(x, Q^2) \right] dx, \quad j = 2, 4, \dots$$

From this expression it is clear that by measuring  $g_1$  and  $g_2$  over all  $x$ , one can obtain direct information about the size of the twist-3 contributions to

nucleon structure. One can also obtain an expression for the leading-twist ( $\tau = 2$ ) contribution to  $g_2$  by setting  $d_j = 0$ , and eliminating  $a_j$  using the equations above. The result, first derived by Wandzura and Wilczek [73], gives the following expression for the twist-2 part of  $g_2$ ,

$$g_2^{ww}(x, Q^2) = -g_1(x, Q^2) + \int_x^1 \frac{g_1(y, Q^2)}{y} dy.$$

### 6.3 Experimental status on $g_2$ and planned measurements

Published data for  $g_2$  were obtained during experiments E142-E155 at SLAC [4], and the SMC experiment at CERN [5]. The world's best data will soon be published from the recent E155x experiment at SLAC, which measured  $g_2$  for proton and deuteron. Using preliminary results from this experiment [74], values for  $g_2$  for the neutron were extracted and are shown in figure 3, along with the earlier SLAC data, the twist-2  $g_2^{ww}$  curve and theoretical model predictions.

It is clear that the data are consistent with the  $g_2^{ww}$  model, but the large errors do not rule out the possibility of significant higher twist effects. Using these data, a value for  $d_2^n$  has been calculated and is shown in figure 9 along with theoretical models: Bag Models [75], QCD Sum Rules [76], Lattice QCD [77], and Chiral Soliton Model [78]. The measured value for  $d_2^n$  is non-zero, and is in disagreement with all of the theoretical calculations. However, in most cases, the disagreement is less than  $1\sigma$ , and the size of the experimental error does not allow one to make a conclusive statement about relative importance of higher-twist effects in the nucleon.

An experiment[79] was planned at JLab next year to make a precision measurement of  $g_2^n$  at selected  $x$  and  $Q^2$  values to have a first clear look at the twist-3 contribution. Figure 10 shows the projected results, which will improve our knowledge of  $g_2^n$  by more than one order of magnitude in precision.

With the future Jlab 12 GeV upgrade, an experiment has been proposed which will make a factor of 10 improvement in the error on  $d_2^n$ . It is important to note that  $d_2$  is dominated by the large- $x$  behavior of  $g_1$  and  $g_2$  due to the factor of  $x^2$  in the integrand. By taking advantage of the high luminosity 11 GeV beam and a new large acceptance spectrometer, precision data for  $g_2$  will be obtained in the range  $0.15 \leq x \leq 0.7$ ,  $W > 2$  GeV, with special

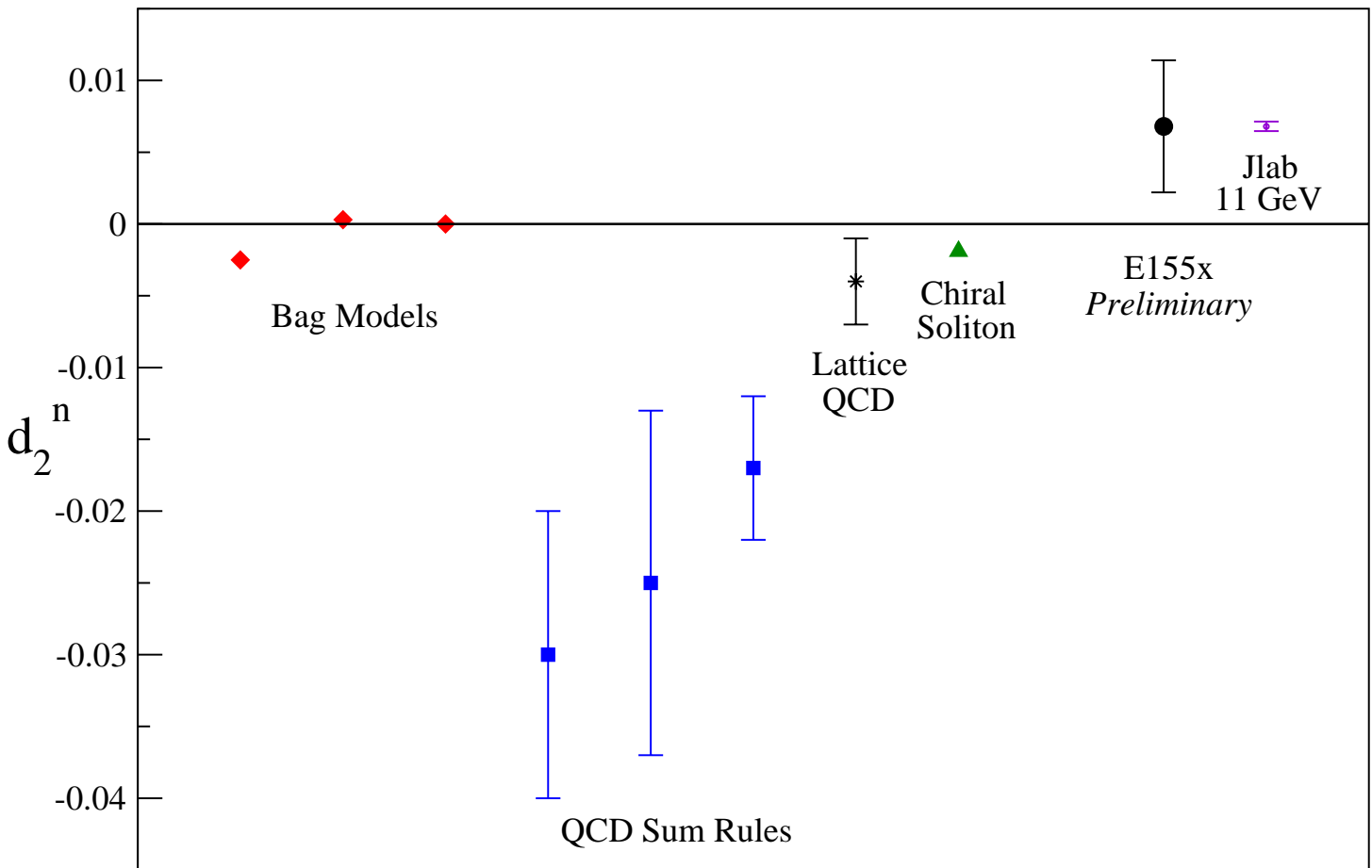


Figure 9: The preliminary result for the twist-3 matrix element  $d_2^n$  from SLAC experiment E155x and Jlab 11 GeV expected result. Also showing are the theoretical predictions.

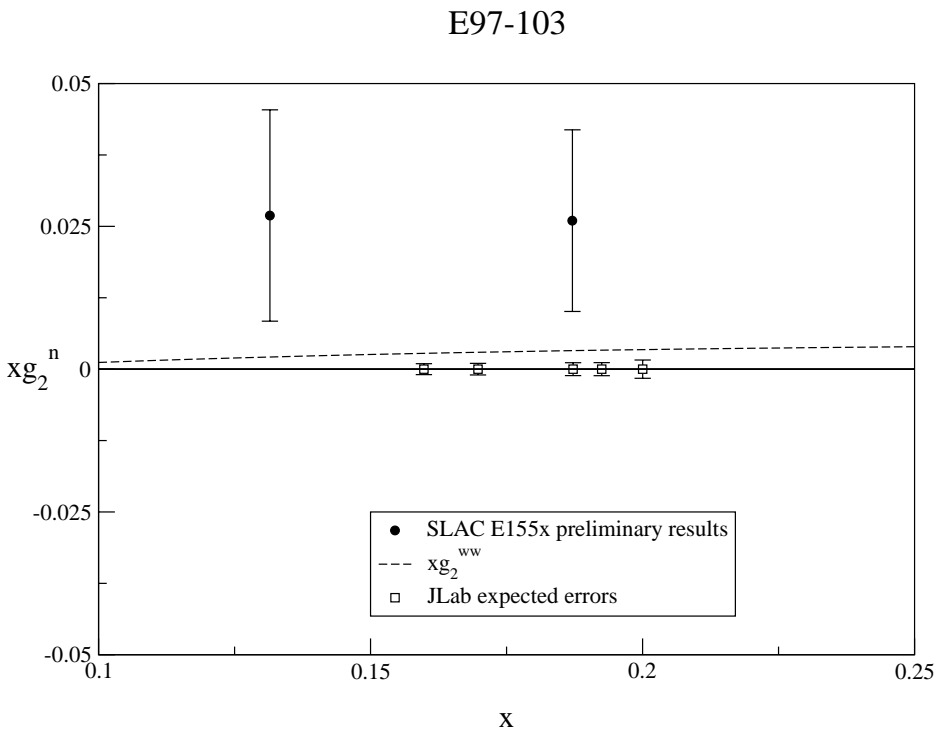


Figure 10: The expected result for the  $g_2^n$  spin structure function from JLab E97-103 comparing with SLAC experiment E155x result

focus on the high  $x$  region which dominates  $d_2$ . In addition, the data will be obtained at *fixed*  $Q^2 = 5 \text{ GeV}^2$  which will eliminate any uncertainty in  $d_2^n$  due to  $Q^2$  dependence. Expected result from this experiment is shown in figure 9.

In addition to  $d_2$ , there is also an important sum rule which can be tested by measuring the  $g_2$  structure function. The OPE formalism does not provide information on the  $j = 0$  moment of  $g_2$ . However, a sum rule derived by Burkhardt and Cottingham (BC sum rule) [80] predicts that this moment goes to zero in the scaling limit,

$$\int_0^1 g_2(x) dx = 0$$

This sum rule was derived using dispersion relations for the virtual Compton amplitudes, and Regge theory to predict the convergence of the dispersion relations. While it is not clear that Regge can be applied here, it is nevertheless important to test this sum rule. Using the SLAC data, the BC sum rule has been measured (E155x preliminary result combined with world data) [74] in the range  $0.02 < x < 0.9$  to have a value of

$$\int_{0.02}^{0.9} g_2^n(x) dx = -0.012 \pm 0.046$$

at an average  $Q^2 = 3 \text{ GeV}^2$ .

The  $g_2^n$  data will be extracted from the recently completed JLab E94-010 and the BC sum rule will be constructed at low  $Q^2$  with an expected improvement of more than one order in precision.

With the 12 GeV upgrade, JLab will study further the BC sum rule at intermediate to high  $Q^2$  with much improved precision, and will be able to study at constant  $Q^2$ .

## 7 Outlook: JLab 12 GeV Upgrade

An upgrade to 12 GeV for Jefferson Lab has already been mentioned in the earlier sections. The CEBAF LINAC has extra space available to add 10 more cryomodules and with some improvement in the cryomodule performance, it will be relatively inexpensive upgrade to reach 11 GeV for the three existing Halls, and with a new hall planned to have additional one half pass, energy will reach 12 GeV. The new hall will be focussed on hadron spectroscopy

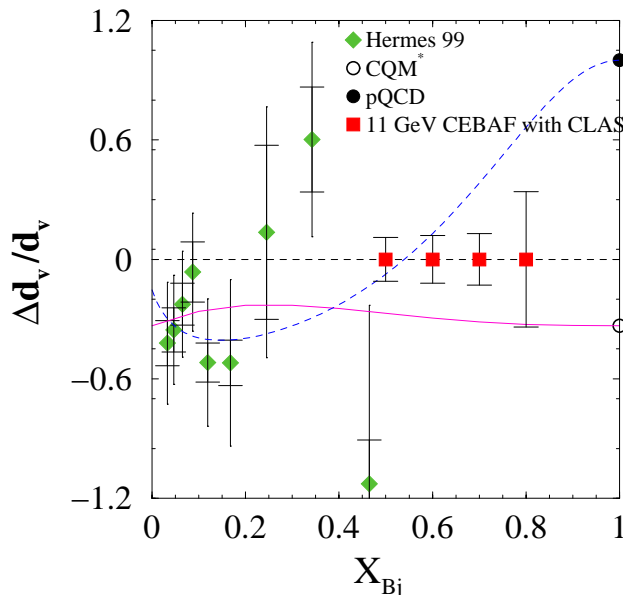


Figure 11: The projected result for the d valence quark spin distribution

study with photoproduction in search of the gluonic degree of freedom and other exotic mesons and baryons. Existing spectrometers and detectors in the other three Halls will be upgraded to match the upgraded accelerator. The energy upgrade will provides a much greater kinematic regime for the deep inelastic scattering and resonance region. There will be an extensive program in nucleon spin structure study.

As have been discussed in the previous sections, we will perform precision measurement of  $A_1^n$  in the high x region and precision measurement of  $g_2^n$  and the moment  $d_2^n$ . A comprehensive study of W and  $Q^2$  dependence study of the spin structure functions  $g_1, g_2$  and  $A_1, A_2$  will be performed on both the proton and the neutron, with emphasize on the valence quark in the high x region.

A new window opens up with semi-inclusive reactions. Spin-flavor decomposition at high x will be done with tagging on the out going pions or keons. An example of expected result on the valence quark spin distribution is shown in figure 11[81]. Sea quark asymmetry[82] and transversity study can also be performed with the upgraded JLab.

Another new physics oppotunity will emerge with deep exclusive scatter-

ing, which will access the newly established theoretical framework of generalized parton distribution. Deep Virtual Compton Scattering and Deep Virtual Meson Production are two examples of experiments being discussed and planned for the 12 GeV upgraded JLab. They may help solve the spin puzzle by providing information on the quark angular momentum contribution to the nucleon spin.

Several workshops were held or are planned to discuss the physics with the JLab energy upgrade. A white paper is being prepared for the long range plan of the US nuclear physics. The JLab 12 GeV upgrade is expected to be in the next 5-year plan. International collaboration is strongly encouraged.

In summary, the ongoing experimental effort will provide us with a wealth of data in the next decade to address many open problems in nucleon spin structure at intermediate distances. To accommodate new physics requirements, an energy upgrade to 12 GeV has been proposed for the CEBAF machine at JLab. This energy upgrade along with the high luminosity and 100% duty factor will provide a much greater kinematic regime for the deep inelastic scattering and resonance region and for semi-inclusive and exclusive processes. We will be in an ever better position to study the nucleon spin structure and strong interaction, especially in the high x region and intermediate distance regime.

This work is supported in part by the U. S. Department of Energy.

## References

- [1] J. Ashman *et al.* (EMC), Nucl. Phys. **B 328** 1 (1989)
- [2] G. Baum *et al.*, phys. Rev. Lett. **45**, 2000 (1980); **51**, 1135(1983)
- [3] R. Jaffe, hep-ph/9207259; hep-ph/9602236; hep-ph/0008038; X. Ji, Phys.Lett. **B309**, 187 (1993); hep-ph/9510362; hep-ph/9610369; X. Chen, D. Qing and F. Wang, Phys.Rev. **C57**, 31 (1998); Phys. Rev. **D58**, 114032 (1998); H. He, Phys.Rev. **D52**, 2960 (1995); hep-ph/9712272; B. Ma, Z. Phys. **A345**, 321 (1993); RIKEN Rev. **28**, 110 (2000);
- [4] P. L. Anthony *et al.* (E142), Phys. Rev. Lett. **71**,959 (1993); Phys. Rev. **D54**, 6620 (1996);  
K. Abe *et al.* (E143), Phys. Rev. Lett **74** , 346 (1995); **75**, 25 (1985);

- 76**, 587 (1996) **78**, 815 (1997); Phys.Lett.**364**, 61 (1995); Phys. Rev. **D58**, 112003 (1998)  
 K. Abe *et al.* (E154), Phys. Rev. Lett **79**,26 (1997); Phys. Lett. **B404**, 377 (1997); P. Anthony *et al.*, (E155), Phys.Lett. **B458**, 536 (1999); hep-ex/9904002; hep-ph/0007248
- [5] D. Adams *et al.*, (SMC), Phys. Lett. **B396**,338(1997); **B357**, 248 (1995); **B 336**, 125 (1994); **B 329**, 399(1994); B. Adeva *et al.*, Phys. Rev. **D56**, 5330(1997)
- [6] K. Ackerstaff, *et al.* (HERMES), Phys. Lett. **B404**, 383 (1997); **B442**, 484 (1998)
- [7] J. D. Bjorken, Phys. Rev. **148**, 1467 (1966); Phys. Rev. **D1**, 465 (1970); **D1**, 1376 (1970)
- [8] S. B. Gerasimov, Yad. Fiz. **2**, 839 (1965).  
 S. D. Drell and A. C. Hearn, Phys. Rev. Lett. **162**, 1520 (1966)
- [9] J. Ellis and R. Jaffe, Phys. Rev. **D10**, 1669 (1974)
- [10] Y. Dokshitzer, Sov. Phys. JETP **46**, 461 (1977); G. Altarelli and G. Parisi, Nucl. Phys. **B126**, 298 (1977); V. Gribov and L. Lipatov, Sov. J. Nucl. Phys **15**, 438, 675 (1972)
- [11] G. t'Hooft and M. Veltman, Nucl. Phys. **B44**, 189 (1972)
- [12] R. Ball, S. Forte and G. Ridolfi, Phys. Lett. **B378**, 255 (1996)
- [13] M. Gluck, E. Reya, M. Stratmann and W. Vogelsang, Phys. Rev. **D53**, 4775 (1996); T. Gehrmann and W. Sirling, Phys. Rev. **D53**, 6100 (1996); E. Leader, A. Sidrov and D. Stamenov, Phys. Rev **D58**, 114028 (1998); Phys. Lett. **B445**, 232 (1998); **B462**, 189, (1999); Y. Goto *et al.*, Phys. Rev. **D62**, 034017 (2000); K. Abe *et al.*, (E154), Phys. Lett. bf B405, 180 (1997); B. Adeva *et al.* (SMC), Phys. Rev. **D58**, 112002 (1998)
- [14] E. Hughes and R. Voss, Annu. Rev. Nucl. Part. Sci. **49**, 303 (1999)
- [15] A. Airapetian, *et al.*, (HERMES) Phys.Rev.Lett. **84**,2584 (2000)
- [16] K. Ackerstaff, *et al.*, (HERMES) Phys. Lett. **B464**, 123 (1999); A. Airapetian, *et al.*, Phys.Rev.Lett. **84**,4047 (2000)

- [17] B. Adeva *et al.*, (SMC), Phys. Lett. **B420**, 180 (1998)
- [18] N. Saito, (RHIC-spin), RIKEN-AF-NP-266 (1996) F. Bradamante, (COMPASS), Prog. Part. Nucl. Phys. **44**, 339 (2000)
- [19] X. Ji, Phys.Rev. **D55**, 7714 (1997); J.Phys. **G24**, 1181 (1998); A. Radyushkin, Phys.Rev. **D56**, 5524 (1997)
- [20] P. Hoodbhoy, X. Ji and W. Lu, Phys.Rev. **D59**, 014013 (1999)
- [21] R. Jaffe, hep-ph/0008038
- [22] F. E. Low, Phys. Rev. 96,1428(1954).  
M. Gell-Mann, M. Goldberger and W. Thirring, Phys. Rev. **95** 1612 (1954).
- [23] I. Karliner, Phys. Rev. **D 7** 2717 (1973).
- [24] R. L. Workman and R. A. Arndt, Phys. Rev. **D 45** 1789 (1992).
- [25] V. Burkert and Zh. Li, Phys. Rev. **D 47** 46 (1993).
- [26] A. M. Sandorfi, C. S. Whisnant and M. Khandaker, Phys. Rev. **D 50** 6681 (1994).
- [27] D. Drechsel, S. Kamalov and L. Tiator, hep-ph/0008306
- [28] L. N. Chang, Y. Liang and R. L. Workman, Phys. Lett. **B329**, 514 (1994).
- [29] S. D. Bass, hep-ph/9703254, 9601244; S. D. Bass, Modern Phys. Lett. A12, 1051 (1997); H.-W. Hammer, D. Drechsel and T. Mart, nucl-th/9701008;
- [30] M. Anselmino, B. L. Ioffe and E. Leader, Sov. J. Nucl. Phys.
- [31] V. Burkert and B. L. Ioffe, Phys. Lett. **B296**,223 (1992).  
V. Burkert and B. L. Ioffe, JETP 105,1153 (1994); **49**,136 (1989).  
D. Drechsel, nucl-th/9411034 (1994).
- [32] J. Ahrens *et al.*, Phys. Rev. Lett., **84**, 5950 (2000)
- [33] H. Olsen and L. C. Maximon, Phys. Rev. **114**, 887 (1959)

- [34] O. Hanstein et al., Nucl. Phys. **A632**, 561 (1999); R. A. Arndt et al., Phys. Rev. **C53**, 430 (1996)
- [35] G. C. Gella, T. R. Hemmert and U.-G. Meissner, Phys. Rev. Lett. **85**, 14 (2000); X. Ji, C. -W. Kao and J. Osborne, Phys. Rev. **D61**, 074003 (2000)
- [36] G. Anton et al., Bonn ELSA Proposal, 1992.
- [37] J. Ahrens et al., Mainz MAMI Proposal A2/1-97
- [38] JLab E91-015, Spokesperson, D. Sober
- [39] JLab E94-117, Spokesperson, J. P. Chen, S. Gilad and C. Whisnant
- [40] A. Sandorfi *et al.*, LEGS-spin Proposal (1994)
- [41] F. Renard, Proceedings of the GDH2000 symposium at Mainz (2000)
- [42] T. Iwata, Proceedings of the GDH2000 symposium at Mainz (2000)
- [43] H. Weller, Proceedings of the GDH2000 symposium at Mainz (2000)
- [44] M. Anselmino, B. Ioffe and E. Leader, Sov. J. Nucl. Phys. 49, 136 (1989)
- [45] V. Burkert and B. Ioffe, JETP, Vol. 105, 1153 (1994)
- [46] D. Drechsel, S. S. Kamalov and L. Tiator, hep-ph/0008306 (2000)
- [47] V. Bernard, K. Kaiser and U-G. Meissner, Phys. Rev. **D48**, 3026 (1993)
- [48] X. Ji and J. Osborne, hep-ph/9905010 (1999)
- [49] X. Ji, C. Kao and J. Osborne, Phys.Lett. **B472**, 1 (2000)
- [50] U-G. Meissner, Proceedings of the GDH2000 symposium at Mainz (2000)
- [51] X. Ji and W. Melnitchouk, Phys.Rev. **D56**, 1 (1997)
- [52] JLab E91-023, Spokespersons, V. Burkert, D. Crabb and R. Minehart
- [53] JLab E93-009, Spokespersons, S. Kuhn and M. Taiuti

- [54] JLab E94-010, Spokespersons, G. Cates, J. P. Chen and Z. E. Meziani
- [55] JLab E97-110, Spokespersons, J. P. Chen, G. Cates and F. Garibaldi
- [56] J. Friar *et al.*, Phys. Rev. **C42**, 2310 (1990); S. Brodsky and J. Primack, Ann. Phys. **52**, 315 (1969)
- [57] C. Ciofi degli Atti and S. Scopetta, Phys. Lett. **B404**, 223 (1997)
- [58] W. Glockle and J. Golak, private communication; G. Salme, private communication; R. Schiavilla, private communication.
- [59] H. Lai, *et al.* (CTEQ5), hep-ph/9903282; A. Martin, R. Roberts, W. Stirling and R. Thorne, Eur. Phys. J. **C4**, 463 (1998); M. Gluck, E. Reya and A. Vogt, Eur. Phys. J **C5**, 461 (1998)
- [60] N. Isgur, Phys. Rev. **D59**, 034013 (1999)
- [61] F. Close, Phys. Lett. **B43**, 422 (1973); Nucl. Phys. **B80**, 269 (1974) and *An introduction to Quarks and Partons* (Academic Press, N. Y., 1979), p. 197
- [62] R. Carlitz, Phys. Lett. **B362**, 352 (1993)
- [63] N. Isgur, G. Karl, Phys. Rev. D23, 817 (1981)
- [64] G. R. Farrar and D. R. Jackson, Phys. Rev. Lett. **35**, 1416 (1975); G. R. Farrar, Phys. Lett. **B70**, 346 (1977)
- [65] S. Brodsky, M Burkhardt and I. Schimidt, Nucl. Phys. **B441**, 197 (1995)
- [66] M. Boglione and E. Leader, Phys. Rev. **D61**, 114001 (2000)
- [67] N. Kochelev, Phys.Rev. **D57**, 5539 (1998)
- [68] JLab E99-117, Spokespersons, J. P. Chen, Z. E. Meziani, P. Souder
- [69] C. Ciofi degli Atti, S. Scopetta, E. Pace and G. Salme, Phys. Rev. **C48**, 968 (1993)
- [70] JLab PR-E00-113, Spokespersons, J. P. Chen, S. Choi and N. Liyanage
- [71] A white paper on JLab 12 GeV energy upgrade (2000)

- [72] R. Jaffe and X. Ji, Phys. Rev. **D43**, 724 (1991)
- [73] S. Wandzura and F. Wilczek, Phys. Lett. **bf B72**, 195 (1977)
- [74] P. Bosted, Proceedings of the HiX2000 workshop (2000), J. P. Chen and Z. E. Meziani, editors.
- [75] X. Song, Phys. Rev. **D54**, 1955 (1996); M. Stratmann, Z. Phys. **C60**, 763 (1993); X. Ji and P. Unrau, Phys. Lett. **B333**, 228 (1994)
- [76] E. Stein, Phys. Lett. **B343**, 369 (1995); I. Balitsky, V. Rarun and A. Kolesnichenko, Phys. Lett. **B242**, 245 (1990); **B318**, 648 (1995); B. Ehrnsperger and A. Schafer, Phys. Rev. **D52**, 2709 (1995)
- [77] M. Gockeler, Phys. Rev. **D53**, 2317 (1996)
- [78] H. Weigel, L. Gamberg, H. Reinhard, Phys. Rev. **D55**, 6910 (1997)
- [79] JLab E97-103, Spokespersons, T. Averett and W. Korsch
- [80] H. Burkhardt and W. Cottingham, Ann. Phys. **16**, 543 (1970)
- [81] T. Forest, Proceedings of the HiX2000 workshop (2000), J. P. Chen and Z. E. Meziani, editors.
- [82] B. Tipton and H. Gao, Proceedings of the HiX2000 workshop (2000), J. P. Chen and Z. E. Meziani, editors.